Investigation of the Surface Glass Transition Temperature by Embedding of Noble Metal Nanoclusters into Monodisperse Polystyrenes

Jörn Erichsen, Jörn Kanzow, Ulrich Schürmann, Kai Dolgner, Katja Günther-Schade, Thomas Strunskus,† Vladimir Zaporojtchenko, and Franz Faupel*

Lehrstuhl für Materialverbunde, Faculty of Engineering, University of Kiel, Kaiserstr. 2, 24143 Kiel, Germany

Received September 4, 2003; Revised Manuscript Received November 24, 2003

ABSTRACT: Chain mobility in a near surface region at a polystyrene/vacuum interface was investigated by embedding of noble metal nanosized clusters. The embedding process was monitored in situ by X-ray photoelectron spectroscopy. The embedding of nanosized clusters needs long-range chain mobility of the polymer. Therefore, the embedding process is a probe for the glass transition in a near surface region. The clusters used in this study are formed by the dewetting of evaporated noble metals onto the polymer surface. First, methodical influences on the embedding process were investigated. An onset embedding temperature T^* was defined. T^* increases with a heating rate comparable to T_g(bulk) determined with a differential scanning calorimeter. Furthermore, T^* increases with nominal metal coverage which results in increasing average cluster radius. The cluster size distribution was investigated by transmission electron microscopy. It is shown that T^* is an upper limit for T_g in a near surface region with a depth of a few nanometers. With optimized probe conditions, embedding processes were performed on monodisperse polystyrene (M_w = 3−1000 kg/mol). The T^* values fit quite well with the Fox−Flory relation, but with a saturation temperature of approximately 8 K below the bulk value. $\Delta T = T_g(\text{bulk}) - T^*$ increases with molecular weight. This molecular weight dependence of T^* will be discussed in terms of several models. The chain end segregation model can be ruled out. To investigate the kinetics of the embedding process, isothermal experiments were performed. From these experiments surface viscosities were derived, which are well below bulk values.

Introduction

Near a surface or interface, the properties of polymers may be altered substantially from those observed in the bulk.[1] The fundamental understanding of polymeric surfaces and films under confinement has become a very important topic within the polymer community during the past decade.[2,3] Mainly monodisperse polystyrenes (PS) were used as a model system. Starting with dewetting studies of PS films on silicon,[4] where a higher chain mobility than in bulk samples was observed, the dynamical properties of polymeric thin films have been analyzed. Thin PS films have a decrease in glass transition temperature (T_g), which depends on the film thickness.[5,6] Thin film means in this context a thickness of the order of the radius of gyration R_g. This decrease in glass transition temperature is much more pronounced for free-standing films.[7] Therefore, the surface plays an important role for the T_g depression of thin films.[3]

Several models and simulations have been performed to describe possible reasons for a near surface zone with enhanced chain mobility. Enrichment of chain ends in a near surface region[8,9] and intrinsic arguments[10,11] were discussed as possible reasons for a surface layer with decreased viscosity. But it is not clear what is the major reason for a near surface zone with enhanced chain mobility. In the past few years several approaches were chosen to characterize the dynamical behavior in a near surface region, but there is still no conclusive picture. Some studies concluded a significant enhancement of chain mobility at the surface[12−22] where, in contrast, others do not observe any differences to the bulk.[23−27] At a first view this may be surprising, but such differences may be due to differences in the depth resolution of the applied method as well as in the heating rate used, in the kind of surface (polymer/vacuum or polymer/air), and finally to the molecular weight used as well as to its distribution.

The methods used for characterization of the surface glass transition can be divided into three larger groups:[3] The first group are divers scanning probe microscopy experiments.[12−14,18,21,23,24] Dependent on the scan mode, and therefore on the information depth, T_g depression was observed or not.[3] Another group are experiments where relaxation of induced surface ordering[26] or roughnesses[17] were observed. The last group are experiments where the embedding of particles was taken as probe for the surface T_g.[15,16,19,20,22,25] In a communication[15] we described the principle of embedding nanoclusters as a way to analyze surface mobility. The embedding was analyzed by XPS[15,16] and also by small-angle X-ray scattering.[25] The clusters used in these studies were formed due to the dewetting of evaporated noble metals onto the polymer surface. The cohesive energy of metals is typically 2 orders of magnitude higher than the cohesive energy of polymers. Furthermore, the interaction between moderately reactive metals and polymers is generally very weak in comparison to the strong metal−metal binding forces. Therefore, metals of low

† Current address: Lehrstuhl für Physikalische Chemie I, University of Bochum, Universitätsstr. 150, 44801 Bochum, Germany.

* Corresponding author: e-mail ff@tf.uni-kiel.de.

10.1021/ma0353080 CCC: $27.50
Published on Web 02/07/2004

reactivity do not wet untreated polymer surfaces. They form clusters during the initial stage of polymer metallization.

Apparently, there is a driving force for embedding of metal clusters; i.e., the Gibbs free energy of a metal particle inside the polymer is lower than that of the particle at the surface. This is related to the high cohesive energy of metals which gives rise to a correspondingly high surface Gibbs free energy of metal particles. The surface Gibbs free energy can be reduced by embedding if the surface tension γ_M of the metal particles exceeds the sum of the interfacial tension γ_{MP} and the polymer surface tension γ_P:[28,29]

$$\gamma_M > \gamma_{MP} + \gamma_P \quad (1)$$

Since the cohesive energy of polymers is so much lower than that of metals γ_P is very small in comparison to γ_M. The embedding of clusters of some nanometers should certainly require long-range chain mobility, which proceeds in experimentally accessible time scales above the glass transition. Therefore, the embedding process reflects to changes in chain mobility in a near surface region.

A similar approach was later performed with colloidal gold clusters.[19,20] These clusters were suspended in deionized water. Therefore, the polymer surface was covered with a water film, which may act as a plasticizer. The embedding of these clusters was observed with an atomic force microscope (AFM) in both studies.

Referring to our previous paper,[15] we have present a detailed study of the embedding process of noble metal nanoclusters into monodisperse polystyrene monitored by XPS. As mentioned above, there are many possible reasons for the controversial results in the literature concerning the chain mobility in a near surface region. Therefore, one aim of this study is to investigate the influence of such properties on the characterization of the surface chain mobility by the embedding process. First, we present the influence of heating rate on the embedding process. Thereafter, we analyze the effect of cluster size reflecting the varying information depth in the near surface region. The cluster sizes, shapes, and distribution were obtained from transmission electron microscopy (TEM). The kinetics of the embedding process were determined in isothermal investigations. Finally, using monodisperse polystyrenes, we analyze the surface glass transition as a function of molecular weight by means of the embedding of small gold clusters.

Experimental Section

Polystyrene (PS) samples with different molecular mass M_w between 3 and 1000 kg/mol from Aldrich Inc. and Polymer Source were used in these experiments. These polystyrenes are terminated with *sec*-butyl groups. The samples are almost monodisperse with $M_w/M_n < 1.08$.

Polystyrene films were prepared by solving the polymer powder in toluene and spin-coating the solution onto polished silicon wafers with their native oxide layer for XPS experiments or onto glass substrates for TEM investigations. The thickness of the films was measured with a profilometer (Stylus DEKTAK 8000, Veeco Ins. Inc.). To rule out the influence of the substrate and polymer film thickness, we used a film thickness of approximately 200 nm for the embedding measurements. This is more than 2 times the radius of gyration R_g for all molecular masses used in this study. Therefore, the influence of the layer thickness on T_g is negligible at this thickness.[1] The samples for the TEM analysis had an approximately film thickness of 80 nm. To be sure that all solvent and water were evaporated and the polymer films were in a relaxed state, all samples were annealed in the UHV system at a temperature $T = T_g(\text{bulk}) + 30$ K for at least 3 h and then cooled to room temperature with a constant cooling rate of 1 K/min prior to evaporation of the metal.

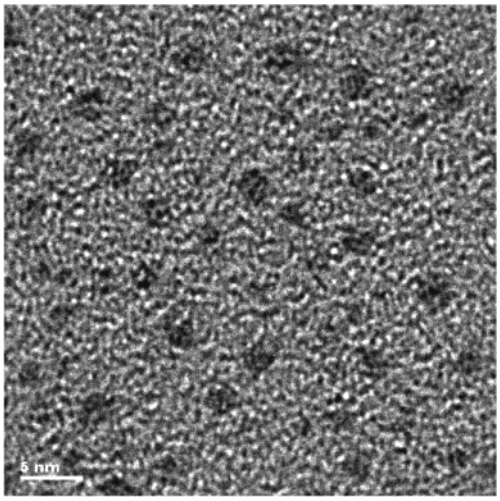

Figure 1. Typical TEM image of a polystyrene film of M_w = 3.5 kg/mol covered with nominal thickness of 0.1 nm Au.

Copper or gold was evaporated onto the polymer surface at room temperature from a heated molybdenum crucible mounted as part of the UHV-XPS system (Omicron Full Lab). The deposition rate and the nominal thickness of the evaporated metal were monitored by a quartz crystal microbalance. The nominal deposition rate was between 0.02 and 0.04 nm/min. During metal evaporation the surface was below 40 °C as determined with an extra thermocouple mounted on the sample surface. This is for all samples far below their glass transition temperature. Dewetting during the annealing can be excluded because both before and after a thermal treatment XPS survey spectra were performed, and no oxygen or silicon signal was observed. If dewetting occurred, then the substrate should be detectable with XPS.

As described in previous papers, noble metals grow as spherical clusters on the polymer surface.[12,13] As a typical example, a TEM image of polystyrene with M_w = 3.5 kg/mol covered with a nominal thickness of 0.1 nm Au is shown in Figure 1. The particles are almost spherical and have a statistical distribution with an average radius $r = 1.2 \pm 0.1$ nm and a layer density of 2×10^{12} cm^{-2}.

For XPS investigations small samples of about 1 cm^2 were broken from a polymer-coated Si wafer. These samples were bonded onto stainless steel sample holders with a graphite glue to increase the thermal contact. To monitor the temperature during the experiment, K-type thermocouples were mounted directly on the sample holder's surface close to the sample. Prior to the measurements, the surface temperature was determined with another thermocouple directly mounted on the surface of a typical sample. For a heating rate of 1 K/min it was observed that the temperature difference between the polymer surface and the thermocouples on the sample holder is always less than 1.5 K. This information was used for calibration of the thermocouple used for the experiments.

XPS measurements were carried out under normal electron emission. The system is equipped with a double anode (VG Microtech XR3E2) and a hemispherical analyzator (VSW Instruments EA 125). The experiments were performed with the Al anode at a typical power of 270 W (15 kV, 18 mA). The spectra were taken with the program SPECTRA. Spectra of the main metal lines and the C 1s line with a pass energy of 100 eV were measured during each series. After a Shirley background correction each peak was integrated. This was performed with the VAMAS data file format processing software CasaXPS. Metal intensities were normalized by the C 1s line to eliminate time-dependent changes in the intensity

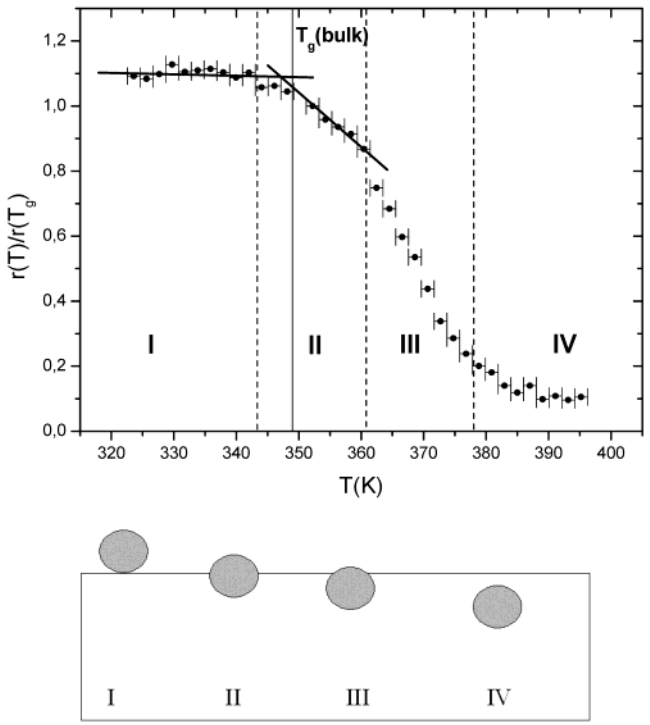

Figure 2. (a) Typical embedding profile of Au cluster on PS with $M_w = 3.7$ kg/mol. The intensity ratio $r(T) = I(\text{Au 4f})/I(\text{C 1s})$ normalized to $r(T_g(\text{bulk}))$ is plotted vs temperature. The embedding profile can be devided into four regions. The normalized ratio decreases around the bulk T_g. Straight lines were fitted to the points in the constant region where no decrease occurs and region of starting decrease, respectively. The intersection point defines the onset embedding temperature T^*. The vertical line marks the bulk T_g determined with DSC. (b) Schematic sketch of the embedding process in the different regions (see text for details).

of the XPS spectra. In the following, the intensity ratio $r = I(\text{metal})/I(\text{C 1s})$ will be analyzed. It was proven that this ratio is independent of any changes in X-ray intensity during the measurement.

To make sure that the X-ray radiation does not affect the results, embedding profiles were recorded with largely different intensities with the same result. Also, detailed spectra with high resolution before and after a run were compared, and no change was observed.

TEM measurements were performed with a Phillips CM 30 microscope at an acceleration voltage of 300 kV. Analysis of the images was carried out with the program Digital Micrograph from Gatan. With this software package also cluster size distributions were determined.

The bulk glass transition of the polymers was determined with DSC (Perkin-Elmer, Pyris 1) with different heating rates using the second run after cooling at 1 K/min.

Results and Discussion

In our earlier paper, we reported the general idea to achieve information about the surface glass transition temperature with the embedding process of noble metal nanocluster. These experiments where performed with constant heating rates.[15]

In the present work, we will first make a definition of an onset embedding temperature, which can be used for characterization of the embedding process.

A typical embedding profile from XPS with a constant heating rate of 0.5 K/min is plotted in Figure 2a for PS with $M_w = 3.7$ kg/mol. The intensity ratio was normalized to the intensity ratio at the bulk T_g value. The latter was determined with DSC. The data points were

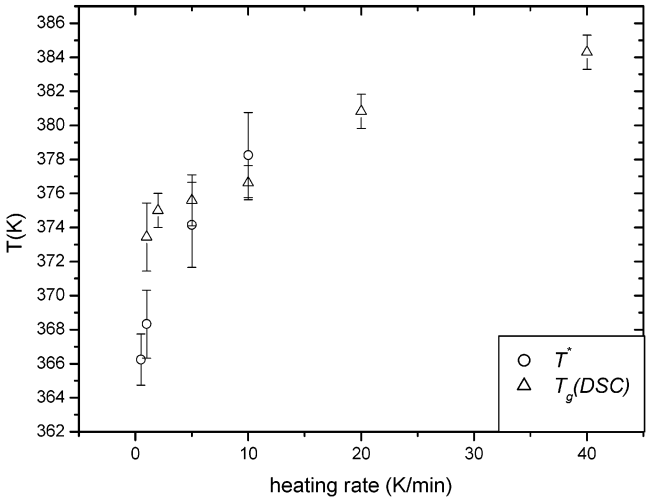

Figure 3. Results of embedding profiles were performed at different heating rates. The determined onset embedding temperature T^* and also T_g(bulk) are plotted vs the heating rate. As bulk glass transition temperature the onset T_g, determined with DSC, was chosen.

put in the middle of the time interval, which is necessary for taking one spectrum. The curve can be divided into four regions: In the first region, the intensity ratio is constant. Thereafter, the ratio starts to decrease with a small slope. Then the decrease accelerates (region III). Finally, the ratio comes into saturation at a ratio of approximately 10% (region IV).

This functionality can be interpreted as following (Figure 2b): At temperatures far below T_g(bulk) the polymer surface has a such high viscosity (region I) that in a typical experimental time scale no long-distance chain mobility and therefore also no embedding occur. Thereafter, the viscosity starts to decrease and long distance chain mobility becomes possible; i.e., clusters start to embed. With decreasing viscosity the clusters embedding becomes faster (region III), and finally the clusters are completely embedded and stay in a region close to the surface (region IV). There is no more driving force for further embedding, and Brownian motion is still very slow.

One could argue that the observed decrease in intensity might be also due to coalescence of small clusters on the surface or other changes in cluster shapes. Therefore, in situ annealing in TEM was performed with 0.1 nm Au on PS with $M_w = 1000$ kg/mol and $M_w = 3.5$ kg/mol. After annealing of more than 3 h at 403 K no difference in cluster size and distribution to the RT values was observed. The decrease in intensity is therefore primarily correlated to the embedding even for a low metal coverage and small clusters.

To analyze the embedding process, we define a temperature T^*. T^* is the intersection point between a linear fit in the region were no embedding occurs (region I) and the beginning embedding process region (region II). T^* can be interpreted as an onset of the embedding process determined by XPS.

As mentioned above, one reason for different results on the T_g(surface) determination may be due to differences in heating rate. Therefore, it is important also for this study to investigate such an influence. For a coverage with 0.5 Å Au on a PS with $M_w = 212$ kg/mol, the embedding process was analyzed as a function of the heating rate (Figure 3). The onset embedding temperature T^* is plotted vs heating rate. For compari-

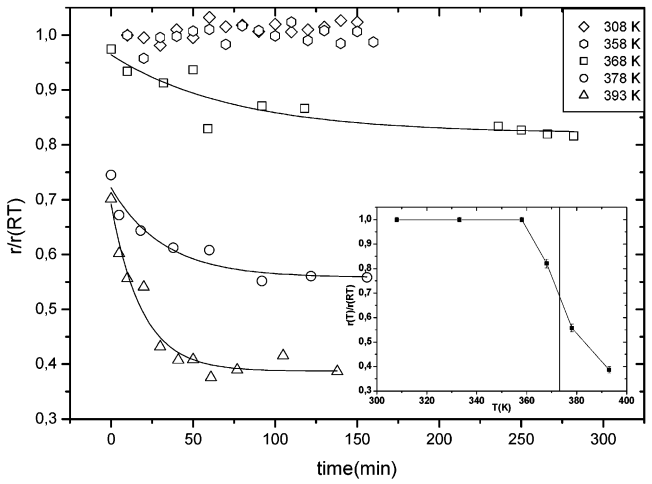

Figure 4. Normalized intensity ratio $r(T)/r(RT)$ with $r = I$(Cu 2p)/I(C 1s) is plotted vs time for different temperatures. The curves are fitted with first-order exponential decays. The saturation values are plotted in the inset. The clusters are embedded well below the bulk T_g, marked by the vertical line.

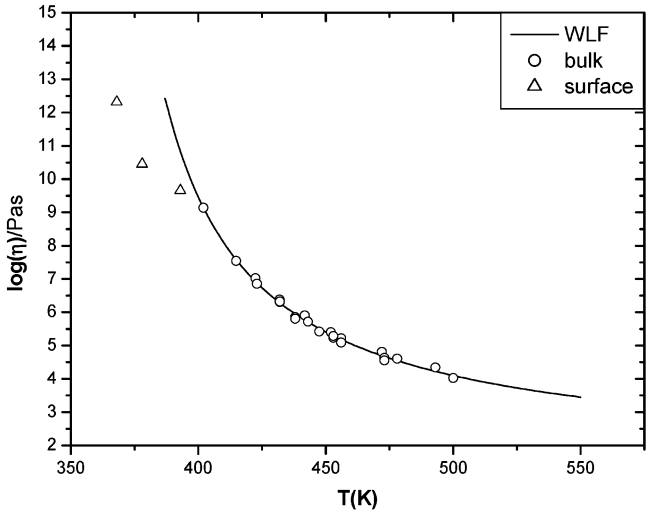

Figure 5. Viscosity derived from the isothermal embedding (Figure 4) is plotted vs temperature. Bulk visocsities are also plotted (from ref 31). A least-squares fit of the WLF equation for the bulk values was performed. The surface values are well below the bulk WLF fit.

son, onset T_g(bulk) values for different heating rates are also included.

T^* increases with heating rate from 366.2 ± 1.6 K for 0.5 K/min up to 378.3 ± 3 K for 10 K/min. The surface values are lower than the bulk ones for small heating rates. The error in measuring T^* increases with increased heating rate due to a reduced number of data points or spectra with lower intensity. This marks a boundary of measuring the T_g(surface) by embedding of nanoclusters at rates above 10 K/min.

Limiting conditions of such heating rate investigations are isothermal experiments. Therefore, experiments were performed at constant temperatures (Figure 4) to obtain a better understanding of the kinetic of the embedding process. Several samples were prepared with a nominal thickness of approximately 0.1 nm copper on PS with M_w = 212 kg/mol. Annealing was performed with a heating step of 5 K/min, and the temperature was then held at the final temperature. The intensity ratio was normalized with its value at RT. The intensity ratio seems to be constant as a function of temperature from RT to 358 K (333 K is not plotted for clarity in the graph). The series at 368 K shows only a slight decrease of the intensity ratio. The samples annealed at 378 and 393 K show a much stronger and faster decrease in intensity. The onset T_g(bulk) was 374 K for this M_w determined with DSC and a heating rate of 1 K/min. This is the same value determined for even thinner films of the same M_w with X-ray reflectivity.[25] First-order exponential decays were fitted through all series. The fitted saturation is plotted vs temperature in the inset of Figure 4. The vertical line marks the T_g(bulk) determined with DSC. T^* has been determined from these saturation values with 361 ± 4 K.

From these isothermal embedding experiments, we derive the viscosity using the embedding model of Kovacs and Vincett:[28,29]

$$\eta = \frac{A_{Cu,PS}t}{a^3 4\pi}\left(\frac{4}{3}x^3 + x^4 + \frac{1}{5}x^5\right)^{-1} \qquad (2)$$

with viscosity η, Hamaker constant $A_{Cu,PS} = 13.5 \times 10^{-20}$ J,[25] cluster radius a, and $x = z/a$ with embedding depth z. t is the embedding time when r/r(RT) reached the plateau. The embedding depth was determined using XPS. The XPS intensity follows $I = I_0 \exp(-z/\lambda)$ with the average depth z and the inelastic mean free path λ = 1.75 nm in PS for the Cu 2P electrons.[30] The embedding process at 368 K yields a viscosity of 2×10^{12} Pa s. This viscosity decreases to 5×10^9 Pa s at 393 K. The logarithm of the viscosity is plotted vs temperature in Figure 5. For comparison, bulk viscosities from the literature[31] are included. Viscosities in the undercooled melt can be described with the WLF equation. A least-squares fit of the WLF equation through the bulk values was performed. One notes that the derived surface viscosities are well below the bulk WLF fit.

Teichroeb and Forrest[20] recently published a work where large gold clusters (d = 10 and 20 nm) were embedded isothermally. They also observed an embedding process which occurs well below the bulk T_g for both cluster sizes. They determined a melt like surface layer with at least 3−4 nm thickness at a temperature at least 7 K below the bulk T_g, which is quite comparable with the isothermal experiments presented in this paper. The main difference to this work is that they used colloidal gold out of a wet process. Our cluster were chosen much smaller of the size of the polymer persistence length to minimize possible effects on the polymer dynamics.

In our previous paper,[15] we embedded Cu cluster into different polymers. In the present study, both Au and Cu clusters are used to examine any possible differences in the embedding process of both metals. Therefore, an experiment was performed, where first Au clusters were embedded. Cu was then evaporated onto the same sample after cooling it down to the room temperature. Afterward, the copper clusters were embedded with the same conditions as for the Au clusters. The intensity ratio is plotted in Figure 6 for an experiment where first the PS were covered with 0.2 nm Au. After heating (0.5 K/min) and cooling (1 K/min) the sample was covered with 0.2 nm Cu. The onset embedding temperature was determined for the Au clusters as T^* = 372.5 ± 1.9 K and for Cu as T^* = 370.9 ± 2.1 K. Therefore, the onset embedding temperature T^* is the same for both metals within the range of error. Hence, it can be concluded that the embedding process

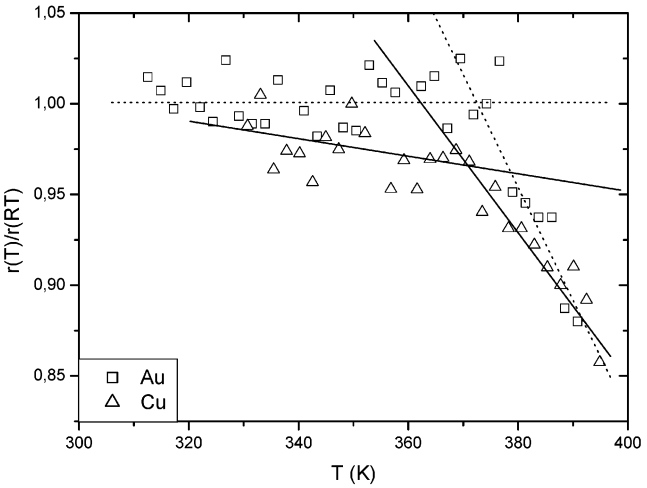

Figure 6. Normalized intensity ratio plotted vs temperature for an experiment where first a nominal coverage of 0.2 nm Au was evaporated onto the PS surface (M_w = 200 kg/mol). After a heating ramp and cooling the same amount of Cu was evaporated onto the surface. The onset embedding temperatures are equal within the error margins.

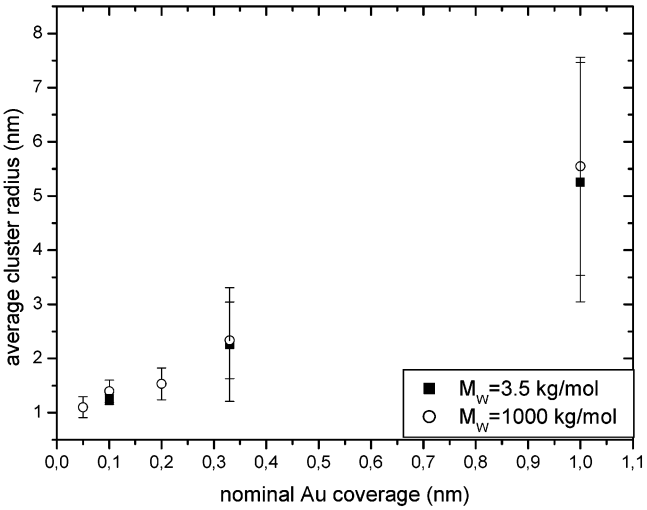

Figure 7. Cluster diameter plotted vs the nominal Au thickness determined by TEM for on PS of M_w = 3.5 kg/mol and M_w = 1000 kg/mol. The cluster sizes increases with nominal coverage. This increase is independent of M_w.

is the same for Au and Cu clusters with comparable sizes because also the Hamaker constants are in the same range.[25] Further, small embedded clusters do not change mobilities of chains at the surface significantly. We have shown that the cluster probe does not influence the polymer dynamics.

As mentioned above, the depth resolution of the applied method may also have a strong influence on the determined chain mobility in a near surface region. Therefore, we investigated the influence of the nominal metal thickness and cluster size on the embedding process.

First, similar samples were prepared for a low (M_w = 3.5 kg/mol) and a high molecular weight (M_w = 1000 kg/mol) PS covered with different amounts of Au. These samples were analyzed with TEM. Cluster size distribution and density were determined from such TEM images. The average cluster radius is plotted vs nominal Au thickness for both molecular weights (Figure 7). The average cluster radius increases with nominal thickness from t = 0.05 nm and $r_c = 1.4 \pm 0.2$ nm to t = 1 nm and

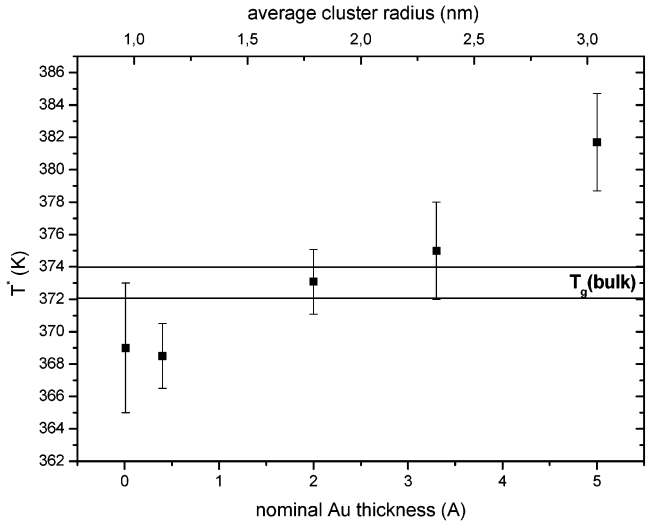

Figure 8. Onset embedding temperature T^* is plotted for different Au coverage on PS (M_w = 1000 kg/mol). T^* increases with nominal thickness. At lowest coverage T^* is determined with a large error because of the low XPS intensity.

$r_c = 5.5 \pm 2.0$ nm. The widths of the radius distribution are so large for 1 nm nominal thickness because of started cluster coalescence. Therefore, theses particles are not spherical anymore. The average cluster radius depends on the nominal Au thickness in the same way for both molecular weights. Furthermore, the density of particles on the surfaces is also the same for both M_w. Deposition of the same amount of gold yields for both molecular weights the same coverage. Therefore, the growth of Au onto polystyrene seems to be independent of the molecular weight although the surface tension of the polymer depends on the molecular weight. However, this dependence is very small for the used molecular weights. Moreira et al.[32] observed surface tensions of monodisperse polystyrene with γ(3.4K)/γ(200K) > 0.96.

The fact that the clusters sizes and distributions are independent of the molecular weight is crucial for the characterization of the surface glass transition in the way used in this study. It ensures that our measuring probe, the nanosized clusters, is the same for all molecular weights.

The embedding process was analyzed with different nominal gold thickness. In Figure 8, T^* is plotted vs the nominal gold thickness on a PS with M_w = 1000 kg/mol with a constant heating rate of 0.5 K/min. The upper x-axis was determined from the average cluster radii measured with TEM (see Figure 7). The onset of the embedding process depends strongly on the Au coverage, which also affects the cluster sizes. T^* increases with nominal Au thickness. For thickness below 0.1 nm well it is well below the bulk T_g. The experiment performed with a nominal thickness of 0.01 nm has an increased error due to the increased statistical noise. For larger nominal thickness and larger average cluster sizes, T^* is around T_g(bulk) or even above this value. This effect has been also observed with small-angle X-ray reflectivity[33] parallel to this study.

Generally, a cluster will not embed if no long-range chain mobility occur beneath the cluster. This is a necessary condition for the embedding process. This holds for all cluster sizes. The observed increase in T^* with cluster size can be accredited to several reasons:

1. For 0.05 nm nominal thickness of Au the resulting cluster radius is approximately $r_c = 1$ nm; this is of the same order of magnitude as the persistence length of PS, which is 1.54 nm.[34] Therefore, these small cluster would affect the mobility of the polymer chain much less than larger ones.

2. Not only cluster sizes increase with nominal thickness but also the relative area of coverage. For 1 nm nominal thickness the coverage is above 0.8. Therefore, the embedding process does not reflect anymore mobilities of the free polymer surface.

3. As mentioned before, the driving force for the embedding is due to the difference of surfaces tension.[28,29] The surface tension of the cluster depends reciprocally on cluster radius. Therefore, smaller cluster have an increased driving force to embed into the polymer surface.

4. Furthermore, the embedding process was observed by XPS under normal emission in this study. Therefor, the clusters must be covered partially with the polymer to detect a decrease in the intensity ratio. Then the metal electrons will be scattered, and therefore the intensity will decrease. This will be the case if the clusters are embedded deeper than their equators. Otherwise, the ratio between metal and carbon line would not change significantly. However, this argument seems to play only a minor rule because such dependence of the embedding process on metal coverage was observed also with another technique.[33]

5. In addition, a surface layer with increased chain mobility was predicted of a few nanometers thickness from measurements on thin films.[2] Direct measurements result in values between 3 and 4 nm thickness of such a layer for $M_w = 214$ kg/mol.[20] If the cluster radius is in this size, only a partial embedding below T_g(bulk) will occur. This would be not detectable with XPS as has been observed even for smaller cluster at nominal thickness of 2 and 3.5 nm. For these coverages the average cluster radius is approximately 1.8 and 2.3 nm, respectively. These cluster radii are below the estimated thickness of a surfaces layer with enhanced chain mobility. For the cluster embedding, enhanced long distance chain mobility is necessary. If a gradient in viscosity exists from the surface to bulk, larger clusters need chain mobility from regions deeper below the surface for the embedding. Therefore, the effective radius, which takes the region into account where enhanced chain mobility is necessary for the embedding, is larger than the cluster radius.

Recapitulating, long-range chain mobility under and beneath a cluster occurs at the onset embedding temperature T^*. By definition, long-range chain mobility sets in T_g . Therefor, T^* marks an upper limit for the glass transition temperature in a near surface region, where enhanced chain mobility is necessary for the embedding process.

In the present light the use of clusters as large as 10−20 nm by Teichroeb and Forrest[20] appears to be disadvantageous because the clusters size is much larger than the polymer persistence length. Hence, the clusters affect the polymer dynamics.

Finally, the influence of molecular weight on the mobility in a near surface region was investigated. T^* is plotted for different molecular weights in Figure 9. For all samples a heating rate of 0.5 K/min and a nominal Au thickness of 0.05 nm were chosen. For comparison, the onset T_g(bulk) measured with DSC is also plotted. The DSC values are linearly extrapolated onset values from series with different heating rates to the low rate used in this experiment. The T^* and the bulk values can be fitted with the Fox−Flory relation[35] $T_g = T_g^\infty - A/M_w$, with $T_g^\infty = 375$ K and $A = 105$ (mol K)/kg with $\chi^2 = 0.7$ for the bulk onset and with $T_g^\infty = 367$ K and $A = 85.5$ (mol K)/kg with $\chi^2 = 2.01$ for the onset embedding values. Not only the saturation temperature T_g^∞ but also the M_w dependence A are significantly smaller for the surface than for the bulk.

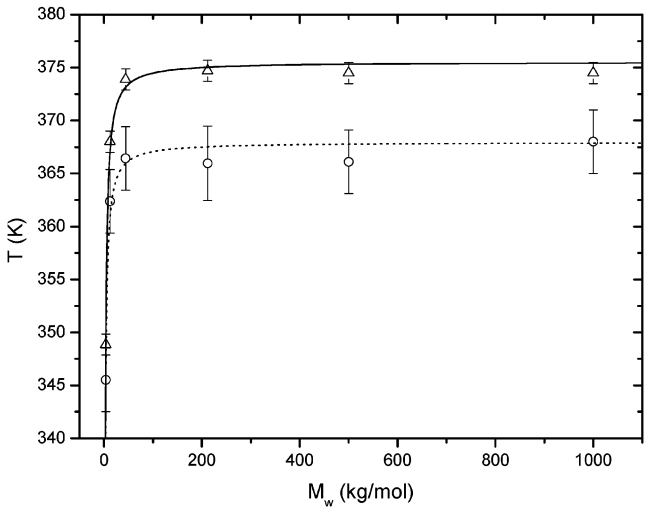

Figure 9. Onset embedding temperature T^* plotted as a function of molecular weight for monodisperse PS films. The heating rate was 0.5 K/min and the nominal thickness 0.05 nm Au. For comparison, T_g(bulk) values are included, which were extrapolated to the heating rate used in the embedding experiments. The Fox−Flory equation was fitted to the data points.

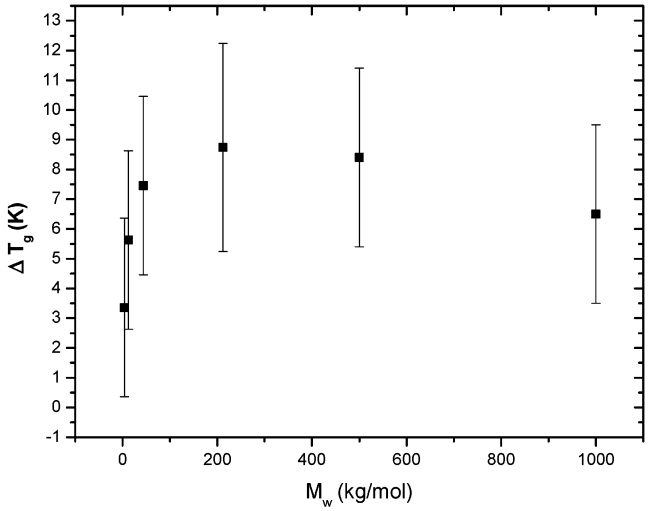

Figure 10. Difference between embedding temperature and T_g(bulk) is plotted vs the molecular weight.

The difference between the surface and the bulk values is plotted in Figure 10 as a function of M_w. The $\Delta T_g = T_g$(bulk) $- T^*$ increases with M_w and seems to come to a saturation above $M_w = 44$ kg/mol. This functional behavior reflects to $\Delta T_g = \Delta T_g^\infty - \Delta A/M_w$.

Mayes[8] developed a model for the enhanced chain mobility in a near surface region. In this model, the enrichment of chain ends is discussed as dominant for a surface zone with enhanced chain mobility. Such an enrichment implicates a strong dependency of ΔT_g on

the molecular weight such that the depression is much more pronounced for lower M_w. Chain end enrichment at the surface will also give rise to an adjacent depletion region below the surface, where the glass transition temperature should be increased compared to that of the bulk.[8] Therefore, a gradient field of chain mobility should exist between both regions. In contrast to the predictions of the chain end enrichment model we observed only a small ΔT_g for low M_w, which increases with M_w and reaches a saturation (see Figure 10). This M_w dependence could still be explained in the chain end enrichment model in two ways: The observed behavior would result if the measuring probe detects different regions in the mobility gradient for different molecular weights. First, this could be the case if the measuring depth was higher for low M_w than for high M_w under the assumption that the mobility gradient is the same for all M_w. It was shown (Figure 8) that larger cluster would effect in an increased T^* and therefore in a decreased chain mobility. Hence, the observed M_w dependence could be explained if the clusters for the low M_w were larger than for the higher M_w's. But it was shown in the TEM investigations that no difference in cluster size occurs between $M_w = 3.5$ and $M_w = 1000$ kg/mol (Figure 7). Therefor, the measuring depth should be constant for all molecular weights, and we can rule out this possibility. Arguing in the chain end enrichment model, a further explanation for the observed M_w dependence could be that the mobility gradient field is not the same for all molecular weights. The extension of the enrichment and the depletion zones below the surface, in which the chain mobility is at most the bulk mobility, are expected to scale with must be in a region with the end-to-end distance R_{ee}. R_{ee} ranges from 7 to over 100 nm for the present polymers. Therefore, an increased mobility gradient is expected for low M_w. However, for our cluster probe radius of only about 1 nm we do not expect any effects from a chain end depression zone below the enrichment zone. Moreover, the postulated magnitude of a T_g depression in the chain end segregation model would implicates a T_g(surface), which is below RT for $M_w < 20$ kg/mol.[8] We would expect a different metal morphology on the polymer surface depending on whether the surface is in the glassy or the rubbery state. In the rubbery state single metal atoms and even small clusters will be embedded into the polymer matrix immediately. These atoms will not be anymore possible centers for cluster nucleation. This would result in different metal cluster morphologies after evaporation for both states. However, the TEM investigations on the metal growth on PS of $M_w = 3.5$ kg/mol and $M_w = 1000$ kg/mol did not show any difference in cluster size and density. Therefor, it can be excluded that the surface of the used low-M_w polystyrene was in the rubbery state during evaporation.

We can conclude that our results are difficult to explain in terms of the chain end enrichment model.

In contrast, the weak M_w dependence observed in this study fits quite well to other models explaining the origin of a surface zone of enhanced chain mobility. Simulations that take into account that chain segments or atoms at the surface are in a different potential than in the bulk yield a higher mobility at the surface both for polymers[10] and for metallic glasses.[11] This intrinsic reason for T_g depression on the surface should have a weaker M_w dependence or vanishing M_w dependence.[3] Furthermore, a comparative study between linear and cyclic polymer chains came to the conclusion that a segregation of chain ends is only a weak contributor to increased chain mobility at free surfaces.[9]

A further origin for the observed increased ΔT_g at higher M_w could be an enrichment of shorter chains at a surface near region. The used polymers are nearly monodisperse, but nevertheless even few shorter chains could affect the T_g at the surface drastically. Therefore, we performed a series of experiments with bimodal mixtures between the lowest and the highest used M_w.[36] These experiments yielded no significant increase of ΔT_g of such mixtures. Therefore, an enrichment of shorter chains in a surface near region can be excluded as a reason for the ΔT_g dependence observed in this study.

Summary

We have studied the embedding of noble metal nanocluster into the surface of monodisperse polystyrenes as a probe for the glass transition in a surface near region. The embedding process was investigated in situ with XPS. First, methodic aspects where analyzed. An onset embedding temperature T^* was defined, which characterizes the beginning of the embedding process. We found that T^* increases with nominal metal coverage and which is accompanied by an increase of the average cluster radius. The cluster sizes were determined with TEM. Furthermore, T^* increases with heating rate similar to the T_g(bulk) does. It was also shown that T^* is the same for Au and Cu clusters of the same size. The onset embedding temperature T^* was shown to be an upper limit for the glass transition in a surface near region.

Also, isothermal embedding was studied to obtain information about the kinetic of the embedding process. Therefrom, viscosity values were calculated and compared with bulk values from literature. The surface viscosity values are well below the WLF fit of the bulk values.

With the optimal cluster size and heating rate, investigations on different monodisperse polystyrenes were performed. T^* can be fitted with the Fox−Flory equation $T_g = T_g^\infty - A/M_w$. Both the T_g^∞ and A are decreased compared with onset bulk values. $\Delta T_g = T_g$(bulk) $- T^*$ increases with molecular weight and saturates above $M_w = 44$ kg/mol with $\Delta T_g \approx 8$ K. The observed M_w dependence can be explained with intrinsic models for a surface region with enhanced chain mobility. Segregation of shorter chains in a surface near region can be neglected to be the origin for the observed M_w dependence.

Acknowledgment. Financial support of the present research by the Deutsche Forschungsgemeinschaft under Project Str 548/5-1 is gratefully acknowledged.

References and Notes

(1) Sanchez, I. C. *Physics of Polymer Surfaces and Interfaces*; Butterworth-Heinemann: Boston, 1992.
(2) Forrest, J. A.; Dalnoki-Veress, K. *Adv. Colloid Interface Sci.* **2001**, *94*, 167.
(3) Forrest, J. A. *Eur. Phys. J. E* **2002**, *8*, 261.
(4) Reiter, G. *Europhys. Lett.* **1993**, *23*, 579.
(5) Keddie, J. L.; Jones, R. A. L.; Cory, R. A. *Faraday Discuss.* **1994**, *98*, 219.
(6) Keddie, J. L.; Jones, R. A. L.; Cory, R. A. *Europhys. Lett.* **1994**, *27*, 59.
(7) Mattsson, J.; Forrest, J. A.; Börjesson, L. *Phys. Rev. E* **2000**, *62*, 5187.
(8) Mayes, A. M. *Macromolecules* **1994**, *27*, 3114.

(9) Doruker, P.; Mattice, W. L. *J. Phys. Chem. B* **1999**, *103*, 178.
(10) Mansfield, K. F.; Theodorou, D. N. *Macromolecules* **1991**, *24*, 6283.
(11) Böddeker, B.; Teichler, H. *Phys. Rev. E* **1999**, *59*, 1948.
(12) Tanaka, K.; Taura, A.; Ge, S. R.; Takahara, A.; Kajiyama, T. *Macromolecules* **1996**, *29*, 3040.
(13) Kaiyama, T.; Tanaka, K.; Takahara, A. *Polymer* **1998**, *39*, 4665.
(14) Satomi, N.; Takahara, A.; Kajiyama, T. *Macromolecules* **1999**, *32*, 4474.
(15) Zaporojtchenko, V.; Strunskus, T.; Erichsen, J.; Faupel, F. *Macromolecules* **2000**, *34*, 1125.
(16) Erichsen, J.; Günther-Schade, K.; Dolgner, K.; Strunskus, T.; Zaporojtchenko, V.; Faupel, F. *Mater. Res. Soc. Symp. Proc.* **2002**, *710*, DD14.5.
(17) Kerle, T.; Lin. Z.; Kim, H. C.; Russel, T. P. *Macromolecules* **2001**, *43*, 3484.
(18) Blizynyuk, V. N.; Assender, H. E.; Briggs, G. A. D. *Macromolecules* **2002**, *35*, 6613.
(19) Rudoy, V. M.; Dement'eva, O. V.; Yaminskii, L. V.; Sukhov, V. M.; Kartseva, M. E.; Orgarev, V. A. *Colloid J.* **2002**, *64*, 746.
(20) Teichroeb, J. H.; Forrest, J. A. *Phys. Rev. Lett.* **2003**, *91*, 016104.
(21) Kawaguchi, D.; Tanaka, K.; Takahara, A.; Kajiyama, T. *Macromolecules* **2001**, *34*, 6164.
(22) Forrest, J. A.; Mattsson, J.; Börjesson, L. *Eur. Phys. J. E* **2002**, *8*, 129.
(23) Pu, Y.; Rafailovich, M. H.; Sokolov, J.; Gersuappe, D.; Peterson, T.; Wu, W.-L.; Schwarz, S. A. *Phys. Rev. Lett.* **2001**, *87*, 206101.
(24) Pu, Y.; Ge, S.; Rafailovich, M.; Sokolov, J.; Duan, Y.; Pearce, E.; Zaitsev, V.; Schwarz, S. *Langmuir* **2001**, *17*, 5865.
(25) Weber, R.; Zimmermann, K.-M.; Tolan, M.; Stettner, J.; Press, W.; Seeck, O. H.; Erichsen, J.; Zaporojtchenko, V.; Strunskus, T.; Faupel, F. *Phys. Rev. E* **2001**, *64*, 61508.
(26) Liu, Y.; Russell, T. P.; Samant, M. G.; Stöhr, J.; Brown, H. R.; Cossy-Favre, A.; Diaz, J. *Macromolecules* **1997**, *30*, 7768.
(27) Kim, H.; Rühm, A.; Lurio, L. B.; Basu, J. K.; Lal, J.; Lumma, D.; Mochrie, A. J.; Sinha, S. K. *Phys. Rev. Lett.* **2003**, *90*, 068302.
(28) Kovacs, G. J.; Vincett, P. S. *J. Colloid Interface Sci.* **1982**, *90*, 335.
(29) Kovacs, G. J.; Vincett, P. S.; Tremblay, C. Pundsack, A. L. *Thin Solid Films* **1983**, *101*, 21.
(30) Tanuma, S.; Powell, C. J.; Penn, D. R. *Surf. Interface Anal.* **1993**, *21*, 165.
(31) Penwell, R. C.; Graessley, W. W. *J. Polym. Sci., Polym. Phys.* **1974**, *12*, 213.
(32) Moreira, J. C.; Demarquette, N. R. *J. Appl. Polym. Sci.* **2001**, *82*, 1907.
(33) Weber, R.; Grotkopp, I.; Stettner, J.; Tolan, M.; Press, W. *Macromolecules* **2003**, *36*, 9100−9106.
(34) Aharoni, S. M. *Macromolecules* **1983**, *16*, 1722.
(35) Fox, T. G.; Flory, P. J. *J. Appl. Phys.* **1950**, *21*, 581.
(36) Erichsen, J.; Shiferaw, T.; Zaporojtchenko, V.; Faupel, F., to be published.

MA0353080